

本資料は2001年07月31日付けで

登録区分変更する。 [大洗工学センター技術情報室]

LOW-CYCLE FATIGUE PROPERTIES OF SUS 304 STAINLESS STEEL
IN HIGH TEMPERATURE SODIUM

Aug., 1977

POWER REACTOR AND NUCLEAR FUEL DEVELOPMENT CORPORATION

Inquiries about copyright and reproduction should be addressed to:
Technical Cooperation Section,
Technology Management Division,
Japan Nuclear Cycle Development Institute
4-49 Muramatsu, Tokai-mura, Naka-gun, Ibaraki 319-1184, Japan

Tel : 029-282-1122
Fax : 029-282-7980
E-mail : jserv@jnc.go.jp

© Japan Nuclear Cycle Development Institute
2001

should be made to it without prior written consent of Power Reactor
and Nuclear Fuel Development Corporation.



PNC SN951 77-03
August, 1977

Low-Cycle Fatigue Properties of SUS304 Stainless
Steel in High Temperature Sodium

Masaatu Hirano*, Kazuyuki Kohashi*,
Shin-ichi Yuhara*, Takashi Nakasuzi*,
and Hideo Atsumo*

Abstract

Strain controlled fatigue tests with triangular waveform in sodium and in air at 550°C were conducted by use of the fatigue test facilities in sodium for the purpose of establishing the fatigue testing techniques and clarifying the fatigue behaviour in sodium.

The results obtained are summarized as follows. The fatigue test technique in high temperature sodium involving the calibration method of the elongation of a specimen and push-pull rod was established.

The fatigue life of SUS304 stainless steel in sodium at 550°C was longer than that in air at the same temperature, at the same strain rate of $1 \times 10^{-3} \text{ sec}^{-1}$ as that of ASME fatigue design curve. Particularly, this tendency was larger as the strain range became lower.

This is the translation, with some additional data and partial revision, of the Report, No. PNC SN943 76-03, issued in February, 1976.

LIST OF FIGURES AND TABLES

- Fig. 1 External appearance of in-air fatigue testing machine
- Fig. 2 External appearance of in-sodium fatigue testing machine
- Fig. 3 Flow sheet of material test sodium loop 2
- Fig. 4 In-sodium fatigue testing machine and test vessel
- Fig. 5a Fatigue test specimen
- Fig. 5b Test specimen for elongation calibration
- Fig. 6 Load waveform
- Fig. 7 The effect of cyclic frequency on the fatigue-crack propagation behaviour of annealed Type 304 at 1000°F. Sawtooth waveform utilized
- Fig. 8 Cyclic load-elongation response (In-sodium and in-air fatigue testing machine)
- Fig. 9 Cyclic load-plastic elongation response (In-sodium and in-air fatigue testing machine)
- Fig. 10 Relation between cyclic load and elongation of specimen
- Fig. 11 Calibration curve (total elongation)
- Fig. 12 Relation between cyclic load and plastic elongation (GL 60 mm and GL 34 mm)
- Fig. 13 Calibration curve (plastic elongation)
- Fig. 14 Hysteresis curve (In air at 550°C, $\epsilon_t = 0.74\%$, $N = 212$, $N_f = 3,013$)
- Fig. 15 Relation between total strain range and cycles to failure
- Fig. 16 Relation between plastic strain range and cycles to failure
- Fig. 17 Comparison of 304 SS (original material and 287-hour exposed materials cycle life in air, helium and high oxygen sodium at 1200°F)

- Fig. 18 Cyclic strain tests - SUS 316 SS sodium, air, and helium
- Fig. 19 Fatigue-crack growth behaviour of annealed Type 304 stainless steel in sodium and vacuum environments at 1000°F (538°C)
-
- Table 1 Main functions of in-air fatigue testing machine
- Table 2 Main functions of in-sodium fatigue testing machine
- Table 3 Chemical composition and mechanical test results
- Table 4 Test conditions
- Table 5 In-sodium fatigue test results
- Table 6 In-air fatigue test results

Low-Cycle Fatigue Properties of SUS304 Stainless Steel in
High Temperature Sodium

C O N T E N T S

1. Introduction
 2. Test facilities
 - 2.1 Facility for fatigue testing in air
 - 2.2 Facility for fatigue testing in sodium
 3. Test specimen and test method
 - 3.1 Test specimen
 - 3.2 Test method
 4. Test results and their examination
 - 4.1 Calibration of elongation
 - 4.2 Fatigue test
 5. Conclusion
- References

1. Introduction

As the operating temperature of reactors rises, the operating conditions for each component have become severer. Particularly in the sodium cooled fast breeder reactor, the hot leg piping of the primary cooling system is operated at such a high temperature range as about 550°C where the effect of creep appears. The recent structural design for such a

high temperature range includes a deformation limitation design method which allows some plastic deformation of the materials considering their creep behaviours, as well as the conventional stress limitation design method.

By this reason, it is urgently needed to accumulate the data on the material behaviours at high temperature, particularly the basic data on creep properties, low-cycle fatigue properties and the creep-fatigue interaction.

Studies of the low-cycle fatigue properties at the high temperature environment have only been conducted under limited conditions and there are available very few fatigue life data for the high temperature structural design. Further, there are almost no data for the material strength behaviour in such a special environment as high temperature sodium.

Such being the case, we conducted in-sodium and in-air low-cycle fatigue tests at 550°C on SUS304 stainless steel which is the main structural material of the sodium cooled fast breeder reactor.

2. Test facilities

2.1 Facility for fatigue testing in air

The facility for fatigue testing in air was manufactured to carry out the fatigue tests in high temperature air and compare the test results with those in high temperature sodium

under the same test conditions. Like the in-sodium fatigue testing machine, this facility is of a closed-loop servo-hydraulic tension/compression type with maximum load capacity of ± 10 tons. LVDT (linear variable differential transformer) and a load cell are used to determine the elongation and the load of the specimen, respectively. Test specimen is heated in a split type electric furnace with a PID controller which can control the surface temperature of the test specimen within the range of $\pm 3^\circ\text{C}$.

Fig. 1 and Table 1 show an external appearance of the in-air fatigue testing machine and its main functions respectively.

2.2 Facility for fatigue testing in sodium

Fig. 2 shows an external appearance of the in-sodium fatigue testing machine.

This facility consists of two corrosion fatigue test loops (CF-11, CF-12) which give the test specimen a high temperature sodium environment, and two in-sodium fatigue testing machines. The outline of the facility will be described, as its details have already been given in a preceding report (1).

As shown in Fig. 3: Flow Sheet, CF loop is the sub-loop of a material test sodium loop 2, consisting of two loops with the similar constitution and function. Sodium is purified by a cold trap in the main loop, heated to the test temperature by two immersion heaters in the CF loop, and then flowed into the test vessel. Sodium in the test vessel is maintained at

the test temperature by means of coil heater on the outer surface of the vessel. Sodium temperature near the test specimen can be controlled within the range of $\pm 2^{\circ}\text{C}$ by the two immersion heaters and the coil heater on the outer surface of the test vessel.

Fig. 4 shows the fatigue testing machine mounted on the test vessel. Main body of the testing machine is hung in the center of the upper cross head and fixed to the loop stand by supporting means. Test specimen is immersed in the liquid sodium with the upper portion fixed by bolts to a push-pull rod via a collar and a keep flange and the lower portion fixed by bolts to the external tube via a collar and a reaction cover. Mounted on the upper portion of the push-pull rod are an actuator, a servo valve, a load cell and an extensometer.

As the extensometer, are equipped differential transformers with the capacities of ± 1 mm and ± 5 mm. In the tests, however, the extensometer with the capacity of ± 1 mm was always used. As the extensometer measures the relative elongation of the push-pull rod to the external tube, the measured values include the sum of the elongation of the push-pull rod and the external tube.

Two in-sodium fatigue testing machines which have the same construction and function are a closed-loop servohydraulic uni-axial tension/compression type with the maximum load

capacity of ± 10 tons. Main functions are similar to those of the in-air fatigue testing machine as shown in Table 2, except for the correction device and an equipment to hold the test specimen under the maximum tensile (compressive) load up to 1000 hours.

3. Test specimen and test method

3.1 Test specimen

Test specimens were made by cutting from SUS 304 plate material with thickness of 40 mm mfd. by the Nihon Yakin Kogyo Co. in Japan. Table 3 shows the chemical composition of the material and the results of mechanical tests.

Fig. 5 shows test specimens for the fatigue test and the elongation calibration. Both specimens are of a round bar type with dimensions of $10\phi \times 30L$ at the parallel portion.

The fatigue test specimen in Fig. 5a was used both for in-air and in-sodium fatigue tests at the temperature of 550°C . In the in-air test, the extensometer is mounted on the flanges at the both ends of the parallel portion to measure elongation of the test specimen. Therefore, the measured result includes the elongation of the shoulder parts between the parallel part and the two flanges. The length of the shoulder parts amounts to 30 mm in total and the elongation at these areas is not negligible.

Test specimen for the elongation calibration has been adjusted to have the minimum shoulders as shown in Fig. 5b for the purpose of obtaining a calibration curve, by means of which the elongation of the parallel part was to be obtained from that of the flange-to-flange part of a fatigue test specimen as shown in Fig. 5a.

By the way, in either specimen, the longitudinal axis is perpendicular to the plate rolling direction, and the surface of the parallel part was finished with #600 emery paper.

3.2 Test method

The fatigue testing machine in sodium is mounted in the test vessel as shown in Fig. 4 and pre-heated to about 300°C. After the pre-heating, the liquid sodium with temperature of about 300°C is filled in the test vessel and heated to and maintained at 550°C by the immersion heaters and the outside coil heater while forced to circulate. The flow rate of sodium flowing into the test vessel is controlled at 2ℓ/min by an electromagnetic pump of the main loop and a flow regulator valve. Sodium level in the vessel is kept constant by adoption of an overflow method and the liquid effluent from the vessel is returned to the main loop and purified by the cold trap. The purification time of the sodium from charge to commencement of the test were about 20 hours including about 3 hours for the pre-heating. The sodium purity was maintained constant

in terms of the cold trap. The cold trap temperature was set at 145°C (oxygen concentration: About 24 ppm), and the purified sodium is supplied to and circulated through the system throughout the test period.

Table 4 shows in-sodium and in-air test conditions. As control method, was adopted a single-axis tension/compression strain control method, and a triangle load waveform as shown in Fig. 6 was used.

It is said that, generally in a high-temperature low-cycle fatigue test, the fatigue life is affected by the strain rate (i.e. cyclic frequency). Particularly in an in-air high temperature test, it is reported that the fatigue life reduces as the cyclic frequency decreases. Fig. 7 shows the result of James' investigation (2) into the effect of the cyclic frequency on the fatigue-crack growth rate of 304 stainless steel (538°C). As shown in Fig. 7, in the in-air test at 538°C, the cyclic frequency has a large effect on the fatigue-crack growth rate. In this test, we adopted the same strain rate of $1 \times 10^{-3} \text{ sec}^{-1}$ as that of the ASME fatigue design curve (3), because the primary purpose of this test was to examine whether the ASME fatigue design curves resulted from the in-air fatigue tests at high temperature are applicable to the design of pipings and components for the use in high temperature sodium.

Fatigue life defined in this paper as N_f refers to the

number of cycles required to produce a load range reduction of 50%.

4. Test results and their examination

4.1 Calibration of elongation

(1) Calibration of elongation of push-pull rod

The total elongation detected at the in-sodium test section is the summation of the elongations of the specimen parallel portion, the specimen shoulder portion and of the push-pull rod. And also that at the in-air test section is the summation of the elongations of the parallel and shoulder portions.

When the respective total elongations, the elongation of the parallel portion, those of the shoulder portions in an in-sodium and an in-air fatigue testing machines subjected to cyclic load and the elongation of push-pull rod in the in-sodium testing machine are assumed to be L_T' and L_T ; L_G' and L_G ; L_R' and L_R ; and L_L , the total elongations L_T' and L_T are expressed by the respective equations (1) and (2) below.

$$L_T' = L_G' + L_R' + L_L \quad (1)$$

$$L_T = L_G + L_R \quad (2)$$

If the same test conditions (temperature, material, shape of test specimen, load, etc.) are adopted in both testing machines, $L_G + L_R$ is equal to $L_G' + L_R'$. Therefore, L_L is the difference between formula (1) and formula (2) (i.e.

$L_L = L_T' - L_T$). Namely, the elongation of the push-pull rod is the difference between the elongations measured by the in-sodium and the in-air fatigue testing machines.

Fig. 8 shows the relation of cyclic load with the total elongation in air and in sodium at 550°C, and Fig. 9 shows the relation of cyclic load with plastic elongation. In Fig. 8, the difference between the total elongation L_T and the plastic elongation L_T' at the same load becomes the elongation L_L of the push-pull rod. In Fig. 9 showing the relation between the cyclic load and the plastic elongation, there is no difference of plastic elongation at the same load between in-air and in-sodium testing machines. This fact shows that elongation of the push-pull rod is an elastic one and that the push-pull rod has a sufficient rigidity as compared with a test specimen with 10 mm diameter. Namely, there is a linear relation between elongation and load of the push-pull rod.

From Fig. 8, the spring constant of the push-pull rod at 550°C is $K_{550} = 3.23 \times 10^2 \text{ton/cm}$.

(2) Calibration of elongation of the parallel portion of the specimen

The elongation (L_T) of a fatigue test specimen measured when cyclic load were applied includes the elongations of the parallel portion (L_G) and the shoulder portion (L_R) of the specimen. If the relation between L_T and L_G at the same

cyclic load is established in advance, the elongation of the parallel portion can be obtained from the measured results in the fatigue test. The calibration is to obtain the relation between the cyclic load and the elongation by measuring a test specimen (for the elongation calibration use) minimized the length of shoulder parts of the fatigue test specimen, and calculate the elongation of the parallel portion at the same load from this relation and that load-elongation relation obtained through measurement of the fatigue test specimen.

Fig. 10 shows the relation between the cyclic load and elongation of a fatigue test specimen (G.L.: 60 mm) and of a calibration specimen use (G.L.: 34 mm). These relations were obtained by the multiple step test in air at 550°C under the test conditions of 550°C strain control, triangle waveform, cyclic frequency of 10 cpm, and 200 step cycles. Load valve on the ordinate was measured at $N = 200$. The elongation of the parallel portion of the specimen can be obtained from these relations. Namely, in the in-air fatigue test, the total elongation of the specimen (G.L.: 60 mm) is measured, but elongation of the parallel portion is not measured. From Fig. 10, however, can be obtained any equivalent elongation of the parallel portion which corresponds to a total elongation of the specimen (G.L.: 60 mm). Fig. 11 shows a calibration curve which represents the relation between the total

elongation of the specimen as a whole (G.L.: 60 mm) and the elongation of the parallel portion obtained from Fig. 10.

Likewise, the elongation of the parallel portion of the specimen in the in-sodium fatigue test can also be obtained from the spring constant of the push-pull rod and the calibration curve in Fig. 11.

Further, an equivalent plastic elongation of the parallel portion corresponding to the total plastic elongation of the specimen can also be obtained in the same manner. Fig. 12 shows the relation between the cyclic load and the elongations of two specimens (G.L.: 60 mm and 34 mm), in which both elongation and load were obtained from the hysteresis curve at $N = 200$. Fig. 13 shows a calibration curve which represents the relation between the total plastic elongation for G.L. = 60 mm and the plastic elongation of the parallel portion.

4.2 Fatigue test

Fig. 14 shows an example of the hysteresis curve at $N = 212$ recorded by a X-Y recorder in an in-air fatigue test ($\epsilon_t = 0.67\%$, $N_f = 3,013$). ϵ_t' in the figure is a constant strain range in the total strain control. ϵ_p' is the plastic strain range, and a residual strain when the load is zero. ϵ_e' is an elastic strain range, and σ_a is stress amplitude. This hysteresis curve is recorded at regular interval during the fatigue test to obtain ϵ_t' , ϵ_p' , ϵ_e' and σ_a . That is recorded during the

in-sodium fatigue test, too.

Figs. 15 and 16 and Tables 5 and 6 show the results of the in-sodium and in-air fatigue tests of SUS 304 stainless steel at 550°C. The tests were conducted with triangle waveform under uni-axial tension-compression strain control at a strain rate $\dot{\epsilon}$ of $1 \times 10^{-3} \text{ sec}^{-1}$.

Total strain range ϵ_t of the test result has been obtained from the hysteresis curve, which was further corrected by the calibration curve in Fig. 11. The plastic strain range ϵ_p was also corrected by the calibration curve in Fig. 13. Both ϵ_p and the stress amplitude σ_a are the values at $Y_2 N_f$. The cycles are defined as the number of cycles when the cyclic load decreased about 1/2 the normal load during the test. (At such time, the testing machine stops automatically.)

Fig. 15 shows the fatigue failure curves of SUS 304 ($\epsilon_t - N_f$ curve) in air and in sodium at 550°C. The ordinate represents the total strain range ϵ_t (%) and the abscissa is the cycles to failure N_f (cycles). Although the $\epsilon_t - N_f$ curve in this figure is not clear since it is few in-sodium test data, the cycles to failure N_f in in-sodium test are generally larger than those in in-air test at the total strain range ϵ_t , from 0.39% to 1.76%. At the higher strain range (about 1.0%), the cycles to failure in the in-sodium test are about 40% larger than those in the in-air test, and the

tendency increases in the lower area of the strain range. Namely, the fatigue life of SUS 304 in sodium at 550°C is longer than that in air at the same temperature, and this tendency is more conspicuous as the strain range decreases.

Fig. 16 shows the fatigue failure curves of SUS 304 in sodium and in air at 550°C at a plastic strain range with the plastic strain range ϵ_p (%) on the ordinate and the cycles to failure N_f (cycles) on the abscissa. Like in the $\sigma_t - N_f$ curve, the cycles to failure of the in-sodium test are also larger than those of the in-air test in this $\epsilon_p - N_f$ curve, and this tendency increases as the plastic strain range decreases.

In Fig. 16, there can be seen a well established exponential relation between ϵ_p and N_f . From Fig. 16, it can also be seen that the Manson-Coffin's equation (3) below is applicable in case of the present in-sodium test at 550°C.

$$\epsilon_p N_f^\alpha = C \quad (3)$$

where α and C : material constants

Values α and C in the above equation are $\alpha_{Na} = 0.466$ and $C_{Na} = 0.221$ in sodium and $\alpha_{air} = 0.621$ and $C_{air} = 0.498$ in air.

Fig. 17 shows the results of strain bending tests on SUS 304 stainless steel in air, in helium and in sodium at 1200°F (649°C) (oxygen concentration: 300 ppm), in which the

in-sodium and the in-air strain curves are crossed at the cyclic strain of about 0.8%, i.e. the fatigue life time in sodium in the higher strain range is longer than that in air, while this relation is reversed in the lower strain range. These test results are different from those of the present tests. In Fig. 18 which shows other test results on SUS 304 in sodium at 1200°F (oxygen concentration: 10 ppm)⁽⁵⁾, however, is seen that the fatigue life in sodium is larger than that in air at the strain range of 0.6 - 2.0% - the same tendency as in the present test results.

Fig. 19 shows the results of James et al's study⁽⁶⁾ of the fatigue-crack growth rate of SUS 304 stainless steel in sodium at 538°C and in vacuum, in which the crack growth rate (da/dN) in sodium at 538°C is smaller than that in air at the same temperature.

In Figs. 15 and 16, the fatigue life of SUS 304 in sodium at 550°C (oxygen concentration: About 24 ppm) is larger than that in air at the same temperature. This seems to be mainly due to the difference between sodium and air environmental conditions, particularly the difference of oxidation degree due to different oxygen concentrations, by reason of a short in-sodium test time (300 hours at longest), in view of the report⁽⁷⁾ that the effects of corrosion, carburization, decarburization and the degraded surface layer by sodium are

small even in the sodium at 525°C (SUS 304, exposure time: 2500 hrs, oxygen concentration: About 12 ppm).

5. Conclusion

Below are the results of strain controlled fatigue life tests conducted in sodium and in air both at 550°C at the oxygen concentration of about 2.4 ppm (cold trap temperature: 145°C) on domestic SUS 304 stainless steel.

- (1) The fatigue test techniques in high temperature sodium including the calibration method for elongation of the specimen, etc. have been established.
- (2) At the same strain range ϵ_t , the fatigue life in sodium at 550°C is larger than that in air at the same temperature, and this tendency increases at lower strain ranges.
- (3) In the plastic strain range ϵ_p also, the fatigue life in sodium is longer than that in air under the same test conditions.
- (4) There is established an exponential relation between the plastic strain range ϵ_p and the cycles to failure N_f in sodium and in air both at 550°C. The value of α in the Manson-coffin's equation is larger in air than in sodium.
- (5) The fatigue life of SUS 304 in sodium at 550°C is longer than that in air at the same temperature because of a difference of oxidation degree between in sodium and in air, considering that there are almost no effects of corrosion, carburization,

decarburization and degraded surface layer in sodium, due to a short in-sodium test time.

It is necessary to perform the following tests in future in order to obtain the basic data for high temperature structure design and clarify the low-cycle fatigue behaviour in high temperature sodium.

1. In-high temperature sodium fatigue tests on SUS 304 stainless steel not exposed in sodium.
2. In-high temperature sodium fatigue tests on SUS 304 stainless steel exposed in sodium.
3. In-high temperature sodium creep-fatigue tests on SUS 304.
4. In-high temperature sodium fatigue-crack growth tests on SUS 304.
6. In-vacuum and in-inert gas fatigue tests on SUS 304.
7. In-high temperature sodium fatigue tests on other materials (SUS 316, Cr-Mo steel, etc.)

References

- (1) Kohashi, Hirano, Yuhara et al.: N 941 75 - 54
"In-sodium Corrosion Fatigue Test (1) Outline of
Test facilities"
- (2) L. A. James "Hold Time Effects on the Elevated
Temperature Fatigue Crack Propagation of Type 304
Stainless Steel" Nuclear Technology Vol. 16 No. 3
(1972)
- (3) ASME B&PV Code Sec III Case 1952.
- (4) MSAR - 67 - 103 (1967)
- (5) L. A. Kirschler et al "A Limited Comparison of
the Mechanical Strength of austenitic Steel in 1200 F
Sodium, Air and Helium" Journal of Basic Engineering
(1969)
- (6) L. A. James et al "Fatigue - Crack Propagation
Behavior of Type 304 Stainless Steel in a Liquid
Sodium Environment" Met.Trans.Vol 6A (1975)
- (7) Atsumo, Maruyama et al.: N 942 72 - 18
"In-sodium Mass Transfer Test on FBR Structural
Materials"

Table 1 Main functions of in-air fatigue testing machine

Type of loading	Uni-axial tension and compression
Maximum load	± 10 tons
Static ram stroke	Max. ± 25 mm
Type of control	Constant strain and constant load control
Cyclic frequency	0.1 - 1,000 cpm
Waveform	Sine, triangle, trapezoid and square waveforms
Extensometer	LVDT (linear variable differential transformer) ± 1 mm
Load cell	Strain gauge type, ± 10 tons

Table 2 Main functions of in-sodium fatigue testing machine

Type of loading	Uni-axial tension/compression
Maximum load	± 10 tons
Static ram stroke	Max. ± 25 mm
Type of control	Constant strain and constant load control
Cyclic frequency	0.1 - 100 cpm
Waveform	Sine, triangle, trapezoid and square waveforms
Extensometer	Linear variable differential transformer ± 1 mm and ± 5 mm
Load cell	Strain gauge type
Hold time	0 - 1000 hours

(Equipped with a strain compensator)

Table 3 Chemical composition and mechanical test results of SUS 304 stainless steel

Analysis	Content wt %															
	C	Si	Mn	P	S	Ni	Cr	Co	Sn	Nb	Ti	Cu	O	B	N	As
Ladle	0.07	0.50	0.92	0.0270	0.0048	99	18.37	0.20	-	-	-	-	-	-	-	-
Product	0.0720	0.51	0.95	0.0290	0.0079	09	18.56	0.20	0.0020	0.0040	0.0010	0.04	0.00920	0.00030	0.0150	0.002

Speci men Size	Y.S. (0.2%) (kg/mm ²)	T.S. (kg/mm ²)	Elong. (%)	Hardness (HB)	Elastic Modulus (kg/mm ²)	Grain Size (ASTM No.)
JIS No. 10 ^{*1} 50	21.8	58.9	69.0	139	2.0 x 10 ⁴	4.0
JIS No. 10 ^{*2} 50	21.8	58.3	68.0	141	-	

*1 Rectangular to the rolling direction

*2 Parallel to the rolling direction

Table 4 Test conditions

Loading type	Uni-axial tension/compression
Control	Constant strain control
Waveform	Triangle waveform
Strain rate	$\sim 1 \times 10^{-3}$ /sec
Strain range	0.39% ~ 1.84%
Cyclic frequency	1.0 cpm ~ 4.0 cpm
Test temperature	550°C

Table 5 In-sodium fatigue test results

Specimen No.	*2 ϵ_t (%)	*1,2 ϵ_p (%)	*1 σ_{α_2} (kg/mm)	Nf (cycles)	f (cpm)	Tf (hrs)
74-23	0.39	0.04	24.5	*3 51,906	3.0	288
74-25	0.70	0.28	28.2	10,247	2.0	85.4
74-26	1.03	0.55	32.7	2,425	1.5	26.9
74-27	1.76	1.17	36.9	564	1.0	9.4
74-28	1.29	0.84	35.9	1,065	1.11	16.0

*1 ϵ_p and σ_{α} are values at 1/2 Nf

*2 ϵ_t and ϵ_p are calibrated values

*3 No failure

Table 6 In-sodium fatigue test results

Specimen No.	*2 ϵ_t (%)	*1,2 ϵ_p (%)	*1 σ_{α} (kg/mm)	Nf (cycles)	f (cpm)	Tf (hrs)
74-31	0.99	0.56	31.2	1,598	2.0	13.3
74-32	0.47	0.16	22.3	8,288	3.75	36.8
74-33	1.47	0.91	34.2	689	1.5	7.7
74-34	0.67	0.32	25.8	3,013	3.0	16.7
74-35	1.01	0.61	30.7	980	2.0	8.2
74-37	1.84	1.23	37.6	275	1.2	3.8
75-1	1.62	1.10	36.6	522	1.5	5.8
75-3	1.63	1.09	37.0	533	1.5	5.9
75-4	1.62	1.10	36.3	435	2.0	3.6
75-5	1.61	1.07	37.1	457	1.0	7.6
75-6	1.04	0.60	31.0	1,285	3.0	7.1
75-7	0.78	0.40	28.4	3,087	4.0	12.9
75-8	2.18	1.56	38.4	299	1.5	3.3

*1 ϵ_p and σ_{α} are values at /2 Nf

*2 ϵ_t and ϵ_p are calibrated values

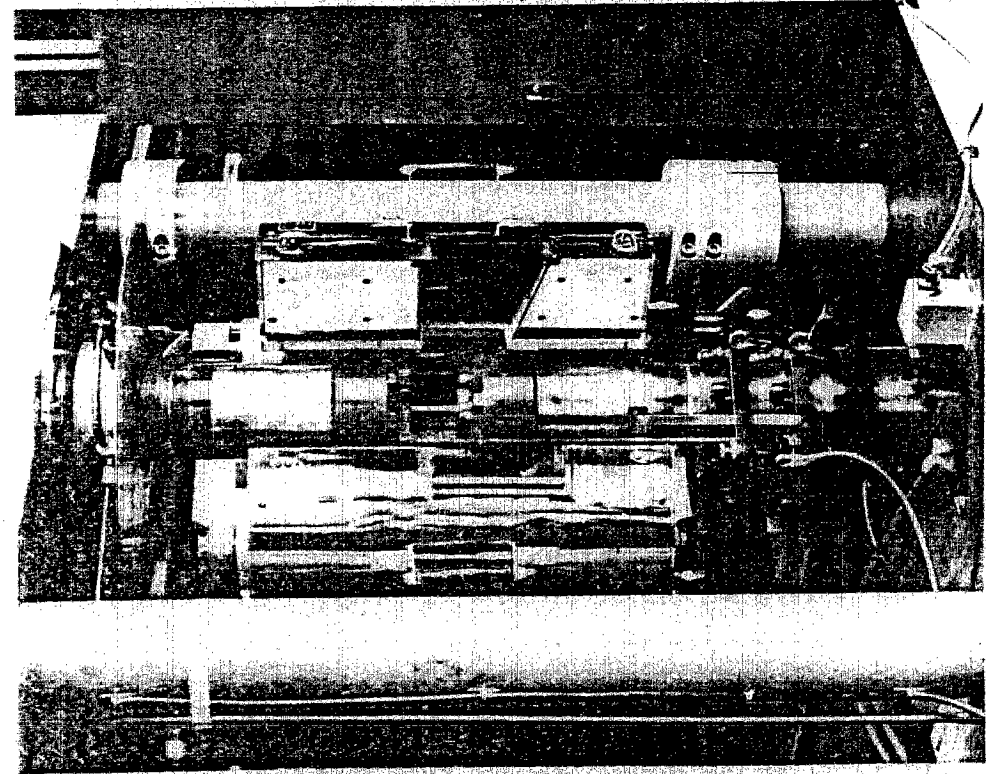


Fig. 1 External appearance of in-air fatigue testing machine

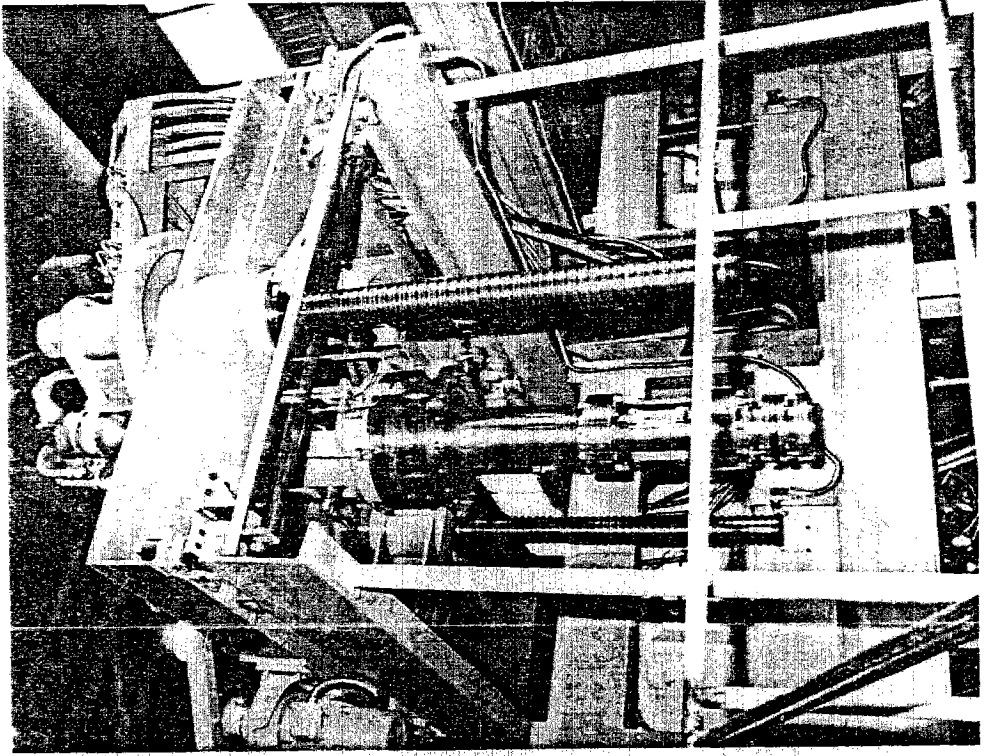


Fig.2 External appearance of in-sodium fatigue testing machine

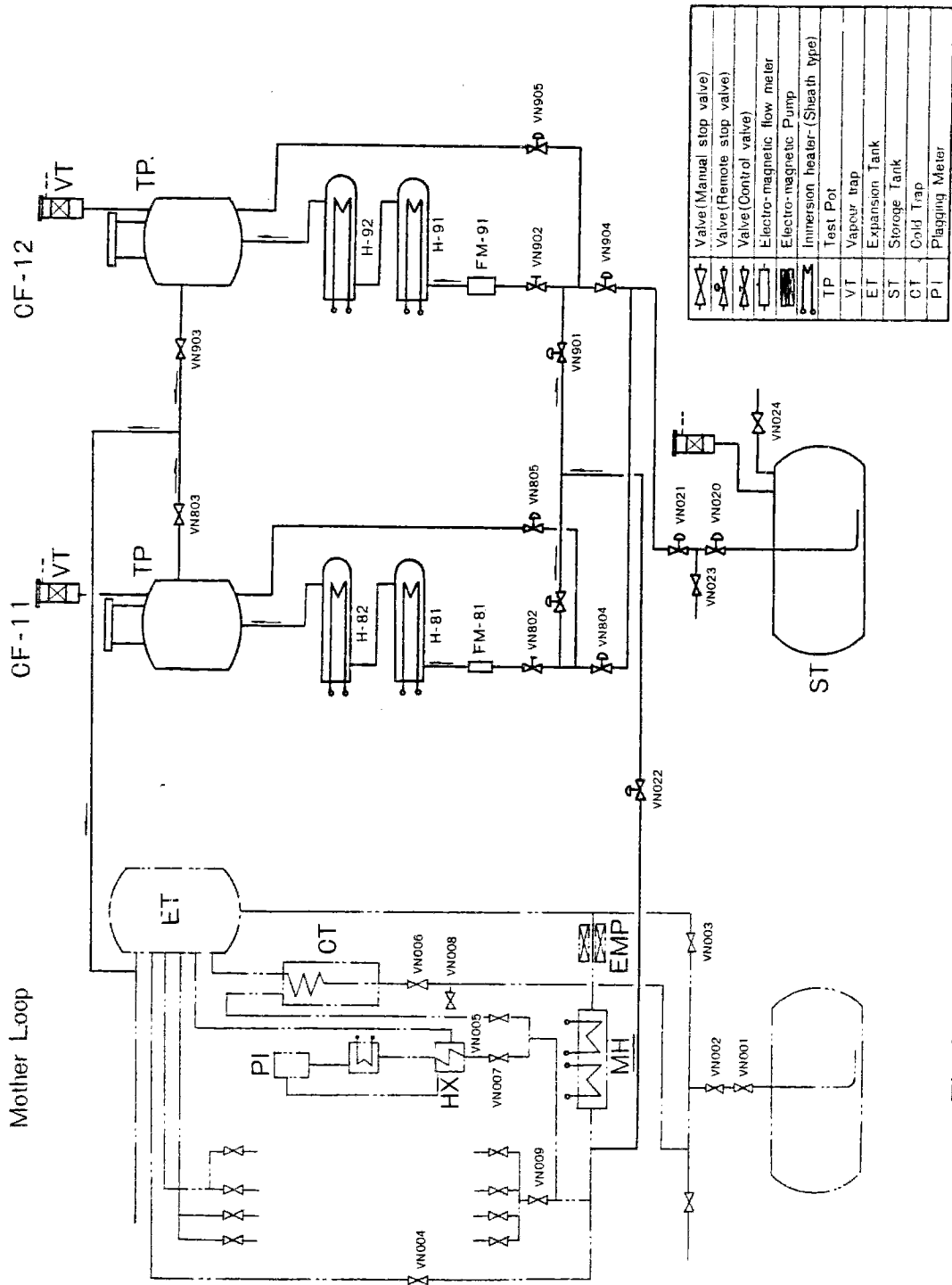


Fig.3 Flow sheet of the Material Test Sodium Loop-2

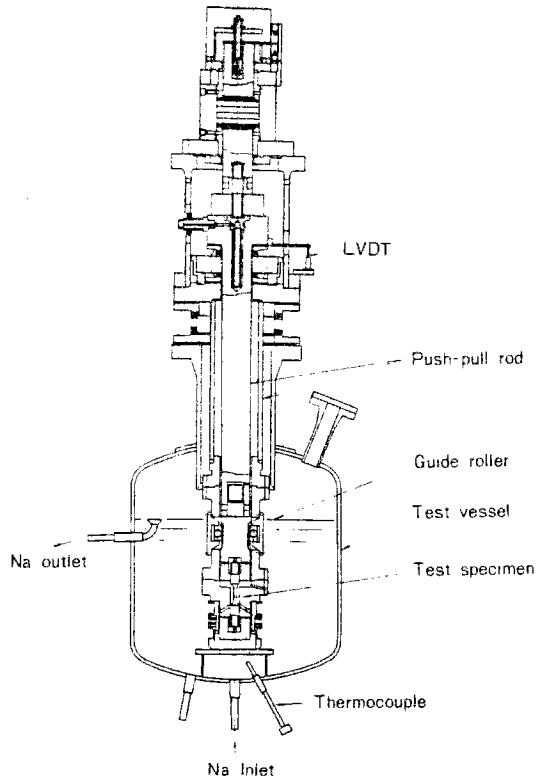


Fig.4 In-sodium fatigue testing machine and test vessel

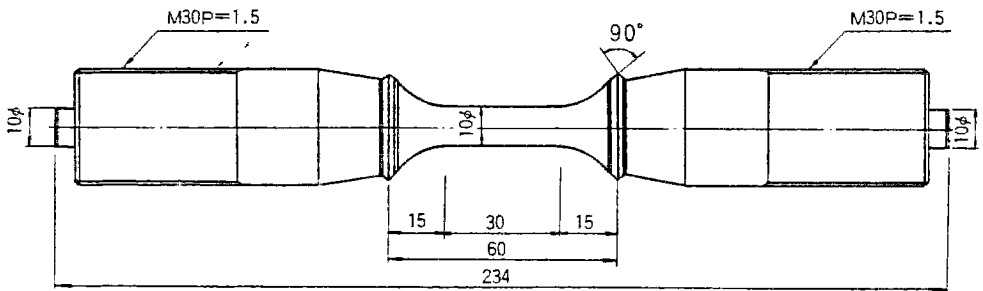


Fig.5.a Fatigue specimen

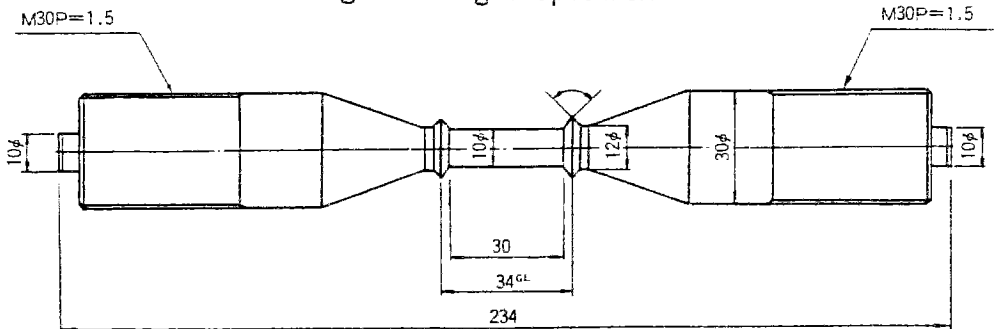


Fig.5.b Calibration specimen

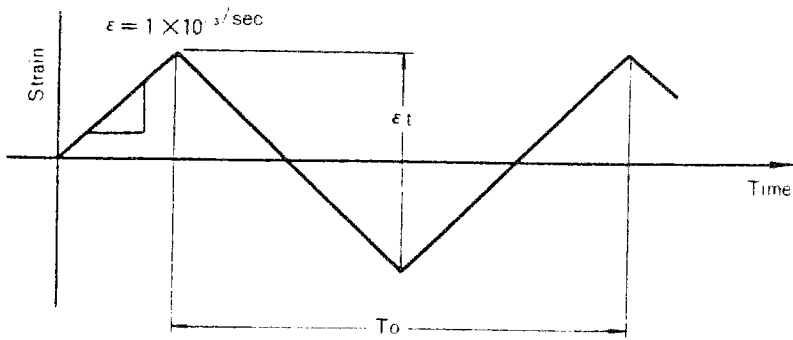


Fig. 6 Load waveform

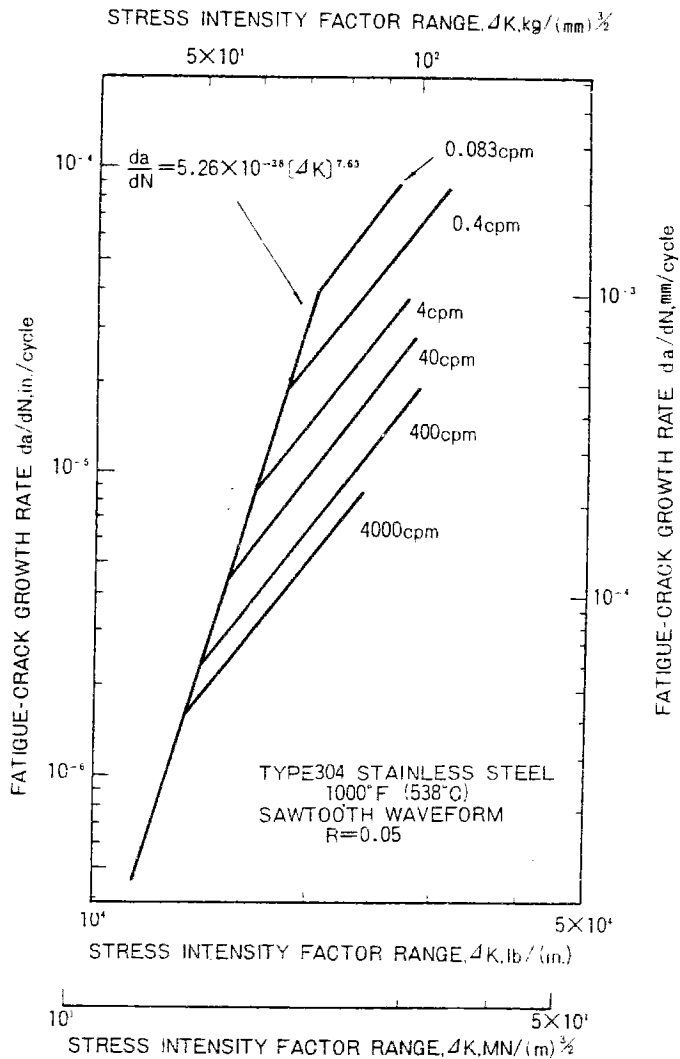


Fig. 7 The effect of cyclic frequency on the fatigue-crack propagation behavior of annealed Type 304 at 1000°F Sawtooth waveform utilized.

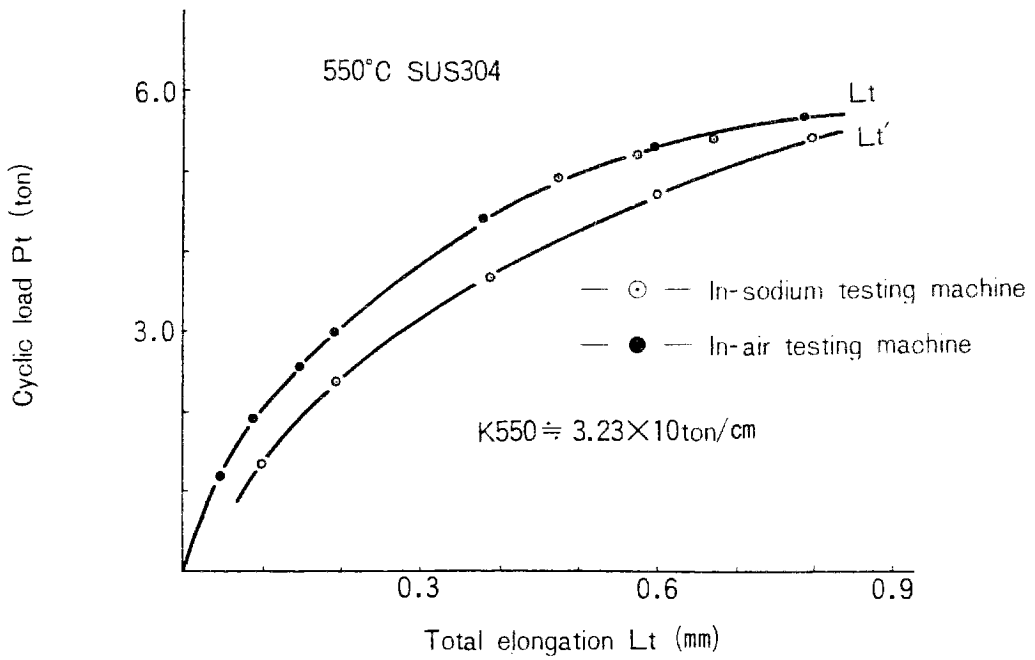


Fig.8 Cyclic load-elongation response (in-sodium and in-air fatigue testing machines)

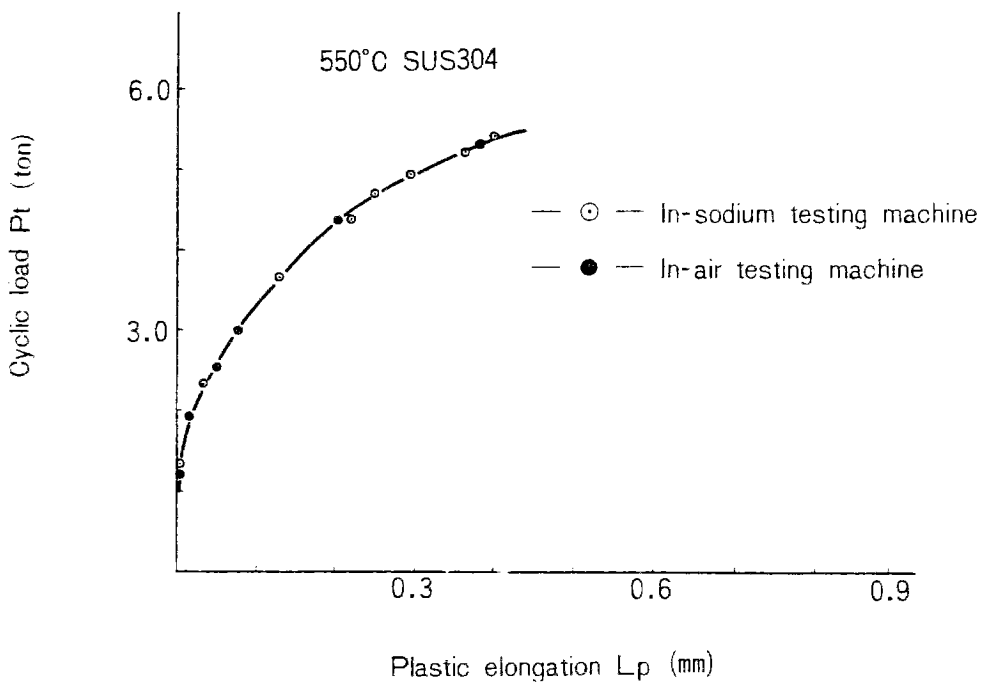


Fig.9 Cyclic load-plastic elongation response in (in-sodium and in-air fatigue testing machine)

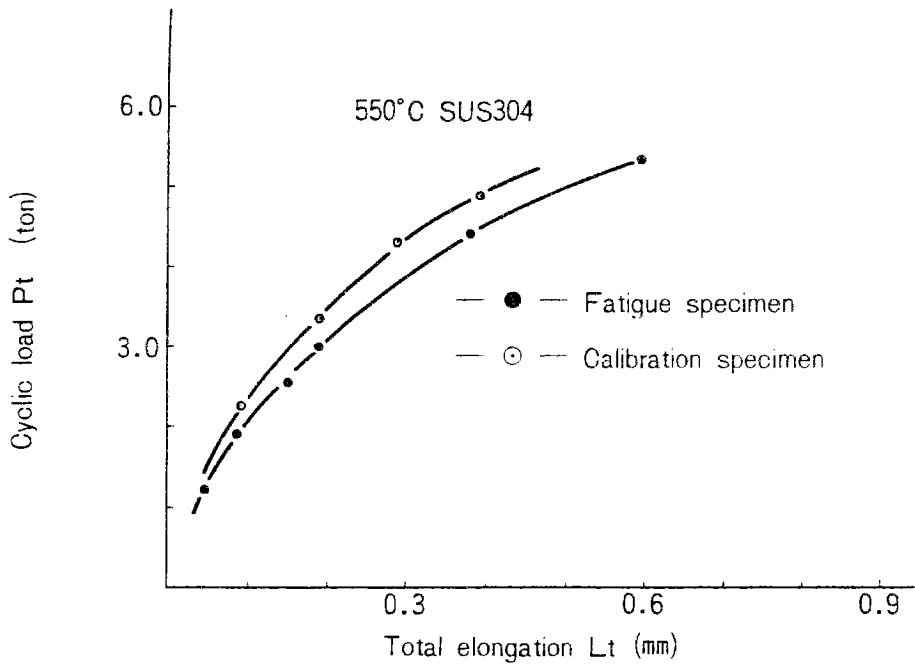


Fig.10 Relation between cyclic load and elongation of specimen (GL60mm and GL34mm)

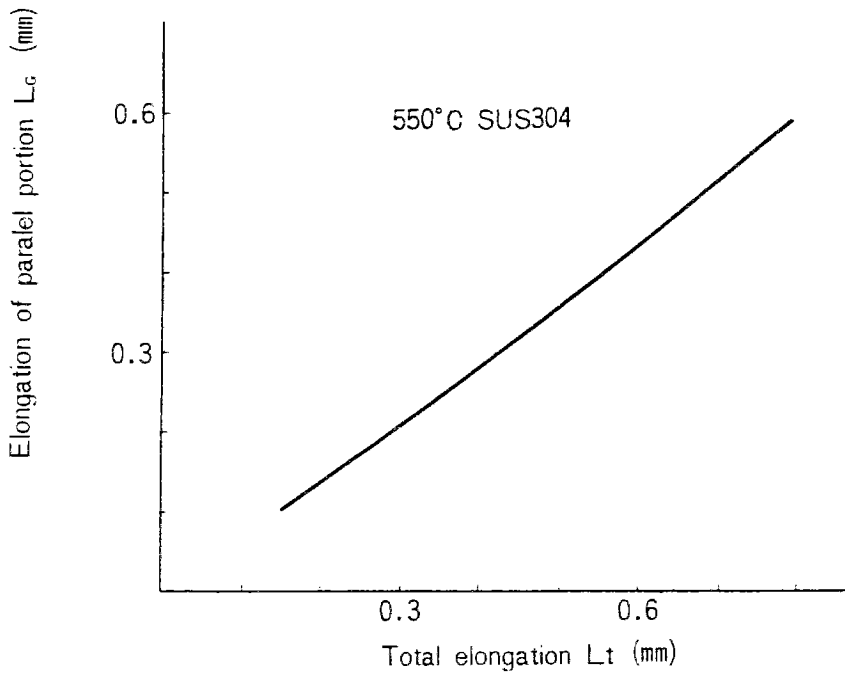


Fig.11 Calibration curve (total elongation)

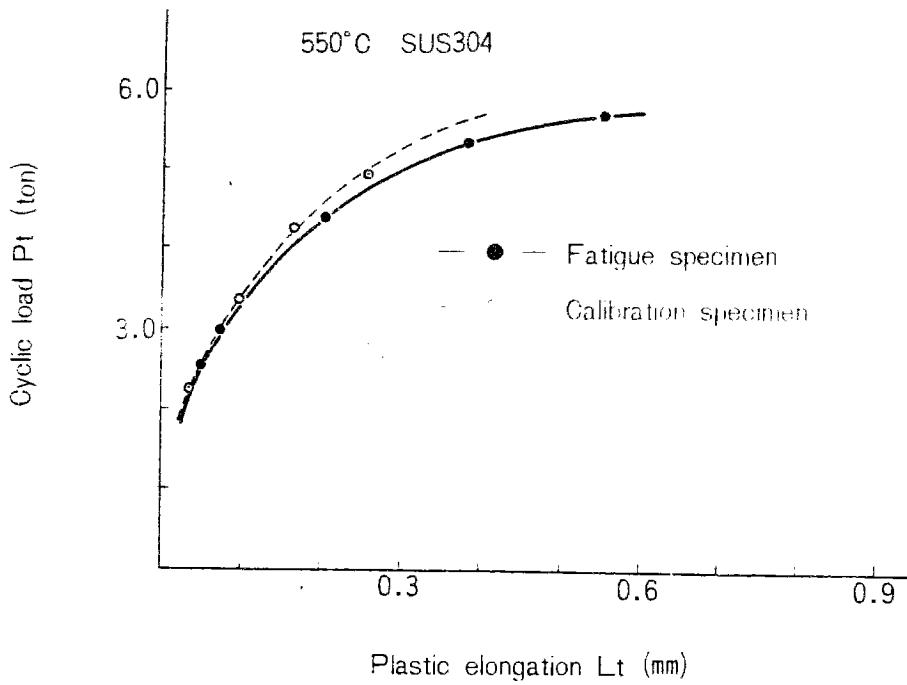


Fig.12 Relation of cyclic load with plastic elongation (GL60mm and GL34mm)

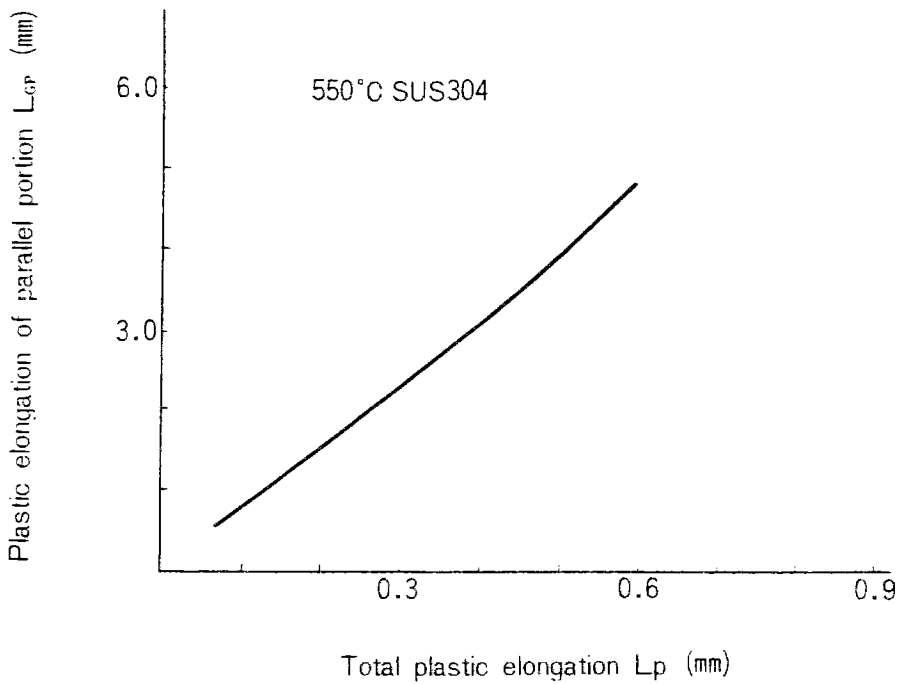


Fig.13 Calibration curve (plastic elongation)

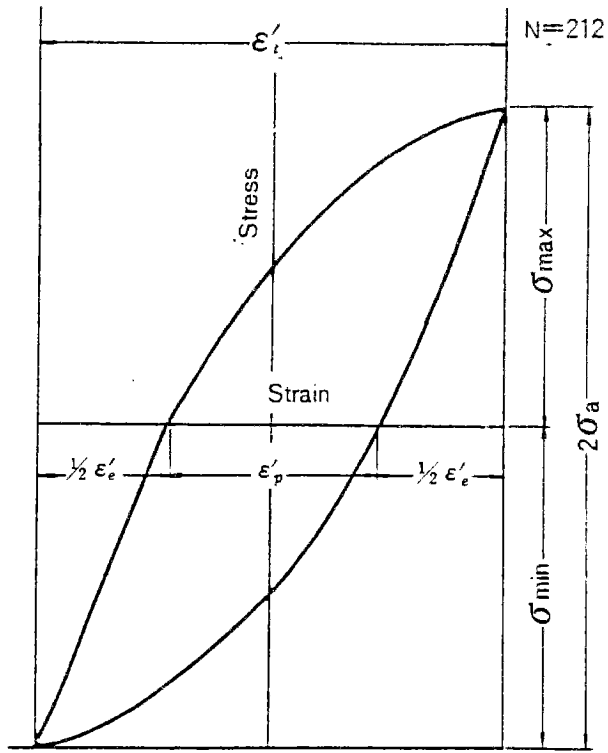


Fig. 14 Hysteresis curve

(In air at 550°C , $\epsilon_t = 0.74\%$, $N = 212$, $N_f = 3.013$)

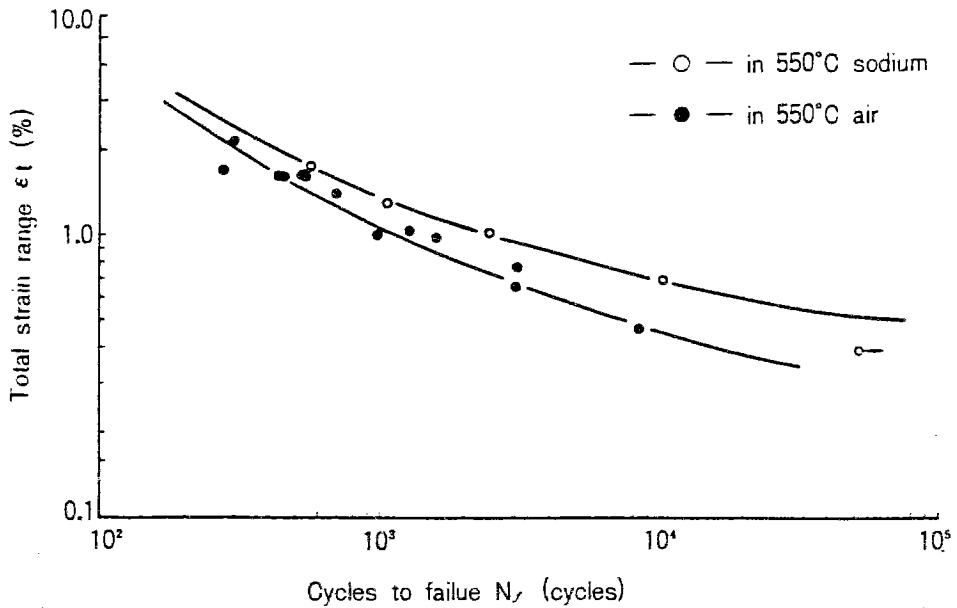


Fig. 15 Relation between total strain range and cycles to failure

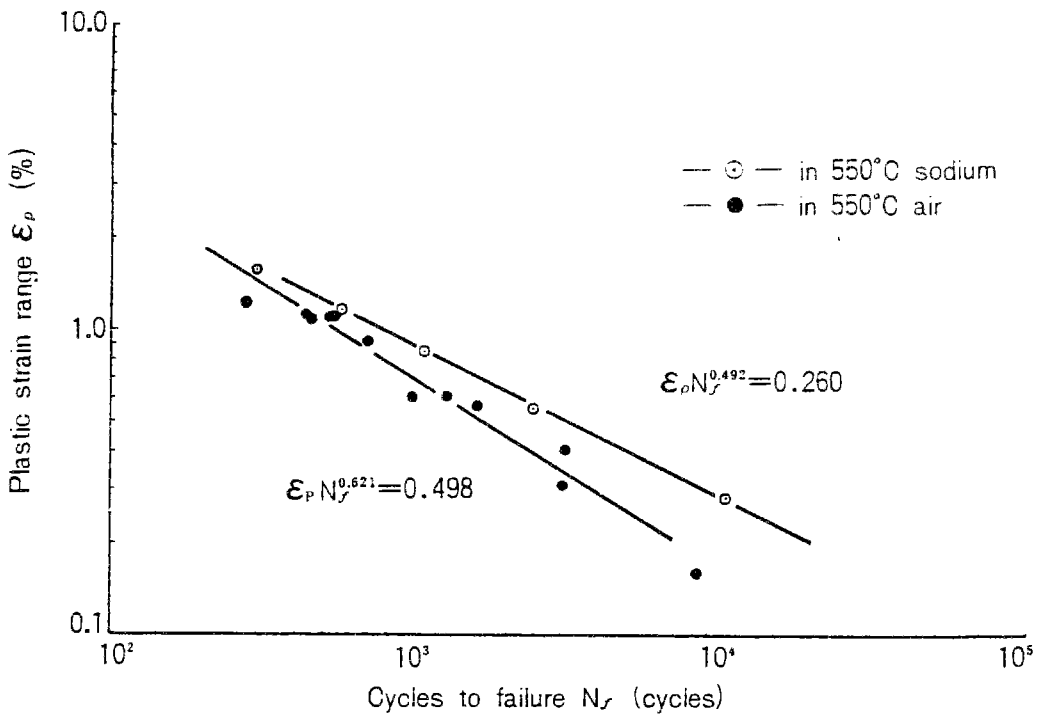


Fig. 16 Relation between plastic strain range and cycles to failure

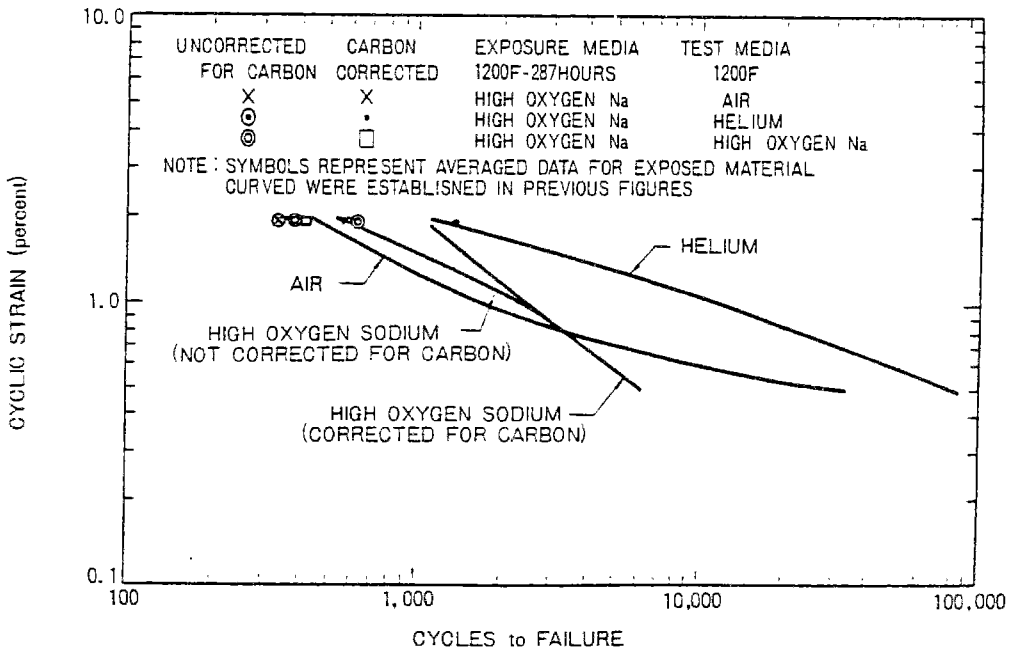


Fig. 17 Comparison of 304SS (original material and 287-hour exposed material) cycle life in air, helium and high oxygen sodium at 1200°F

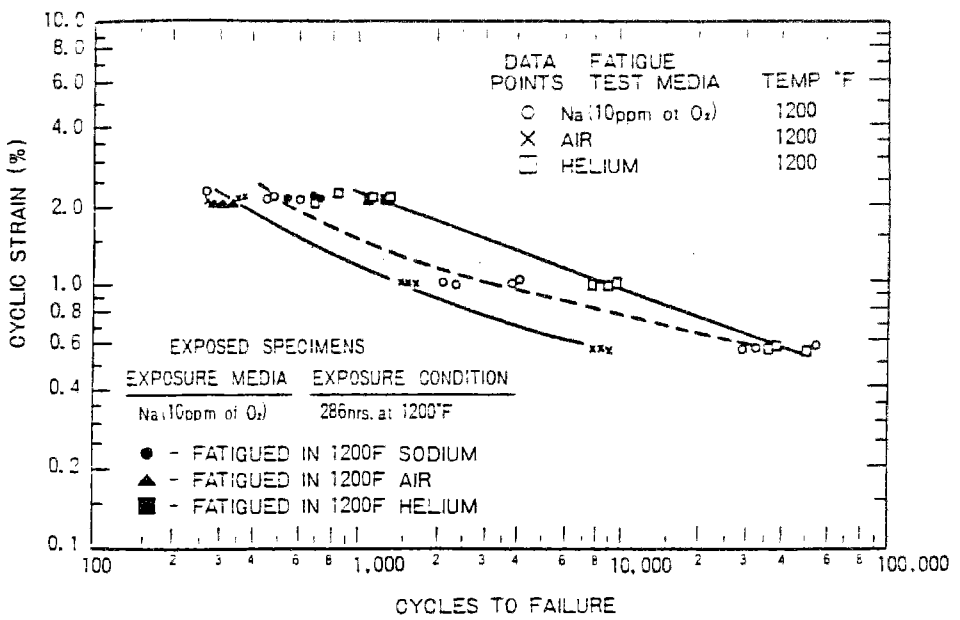


Fig. 18 Cyclic strain tests-316ss sodium, air, and helium

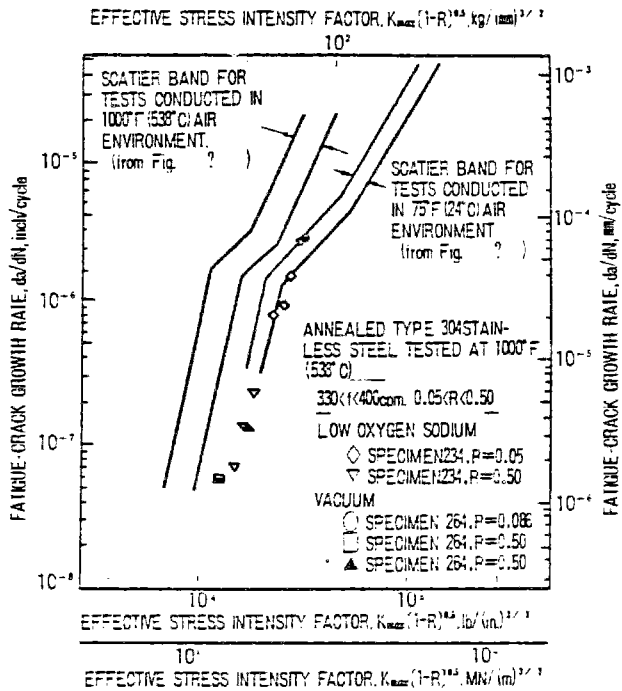


Fig. 19 Fatigue-crack growth behavior of annealed Type 304 stainless steel in sodium and vacuum environments at 1000°F (538°C)